Received: 23 August 2022 | Revised: 21 October 2022 | Accepted: 3 November 2022

DOI: 10.1111/mec.16772

FROM THE COVER

MOLECULAR ECOLOGY WILEY

Conspicuous coloration of toxin-resistant predators implicates additional trophic interactions in a predator–prey arms race

Michael T. J. Hague[1] | Lauren E. Miller[2] | Amber N. Stokes[3] | Chris R. Feldman[4] | Edmund D. Brodie Jr[5] | Edmund D. Brodie III[2]

[1]Division of Biological Sciences, University of Montana, Missoula, Montana, USA

[2]Department of Biology, University of Virginia, Charlottesville, Virginia, USA

[3]Department of Biology, California State University, Bakersfield, California, USA

[4]Department of Biology, University of Nevada, Reno, Nevada, USA

[5]Department of Biology, Utah State University, Logan, Utah, USA

Correspondence
Michael T. J. Hague, Division of Biological Sciences, University of Montana, 32 Campus Dr. HS 104, Missoula, MT 59812, USA.
Email: michael.hague@mso.umt.edu

Funding information
Division of Environmental Biology, Grant/Award Number: 1601296 and 1911485; Division of Integrative Organismal Systems, Grant/Award Number: 1355221

Handling Editor: Kayla King

Abstract

Antagonistic coevolution between natural enemies can produce highly exaggerated traits, such as prey toxins and predator resistance. This reciprocal process of adaptation and counter-adaptation may also open doors to other evolutionary novelties not directly involved in the phenotypic interface of coevolution. We tested the hypothesis that predator–prey coevolution coincided with the evolution of conspicuous coloration on resistant predators that retain prey toxins. In western North America, common garter snakes (*Thamnophis sirtalis*) have evolved extreme resistance to tetrodotoxin (TTX) in the coevolutionary arms race with their deadly prey, Pacific newts (*Taricha* spp.). TTX-resistant snakes can retain large amounts of ingested TTX, which could serve as a deterrent against the snakes' own predators if TTX toxicity and resistance are coupled with a conspicuous warning signal. We evaluated whether arms race escalation covaries with bright red coloration in snake populations across the geographic mosaic of coevolution. Snake colour variation departs from the neutral expectations of population genetic structure and covaries with escalating clines of newt TTX and snake resistance at two coevolutionary hotspots. In the Pacific Northwest, bright red coloration fits an expected pattern of an aposematic warning to avian predators: TTX-resistant snakes that consume highly toxic newts also have relatively large, reddish-orange dorsal blotches. Snake coloration also seems to have evolved with the arms race in California, but overall patterns are less intuitively consistent with aposematism. These results suggest that interactions with additional trophic levels can generate novel traits as a cascading consequence of arms race coevolution across the geographic mosaic.

KEYWORDS
aposematism, arms race, coevolution, geographic mosaic theory, tetrodotoxin

1 | INTRODUCTION

Antagonistic coevolution between natural enemies is thought to be a major driver of the evolution of biodiversity (Dawkins & Krebs, 1979; Ehrlich & Raven, 1964; Vermeij, 1987; Zaman et al., 2014). Arms race coevolution between natural enemies like predator and prey or herbivore and plant is characterized by escalation and counter-escalation at the phenotypic interface of coevolution—the traits of each species that mediate antagonistic interactions (Brodie III & Brodie Jr., 1999; Brodie III & Ridenhour, 2003). This process of reciprocal

Michael T. J. Hague and Lauren E. Miller are co-first authors.

selection can lead to the evolution of highly exaggerated traits, such as prey toxicity and predator resistance (Hanifin et al., 2008; Reimche et al., 2020; Toju et al., 2011; Toju & Sota, 2005). In the geographic mosaic theory, coevolutionary hotspots are defined as locations where reciprocal selection occurs at the phenotypic interface (Thompson, 1999, 2005). The spatial distribution of hotspots, combined with the effects of population structure, can generate a geographic mosaic of coevolution across the landscape (Benkman et al., 2003; Hague et al., 2020a; Thompson, 1999, 2005; Toju et al., 2011; Zangerl & Berenbaum, 2003). Coevolutionary hotspots may also generate cascading effects, as organisms with exaggerated armaments may experience novel selection pressures that were not directly involved in the pairwise arms race interaction. For example, many insect herbivores have evolved resistance to defensive toxins in plants and, as a consequence, they have also evolved the ability to sequester these toxins as a defence against their own predators (Dobler et al., 2012; Groen & Whiteman, 2021; Opitz & Müller, 2009; Petschenka et al., 2022). In this respect, coevolution can have cascading consequences that drive the evolution of novel traits along related axes of variation, which may involve other levels of trophic interaction.

We investigated whether such cascading effects arise within the context of a geographic mosaic of coevolution, where hotspots (and coldspots) of coevolution are interspersed across the landscape (Thompson, 1999, 2005). Common garter snakes (*Thamnophis sirtalis*) have evolved extreme resistance to tetrodotoxin (TTX) in a geographic mosaic of arms race coevolution with their deadly prey, Pacific newts (*Taricha* spp.) (Brodie III & Brodie Jr., 1990; Brodie Jr. et al., 2002; Hague et al., 2017, 2020a; Hanifin et al., 2008). Phenotypic TTX resistance is tightly correlated with levels of newt TTX across western North America (Brodie Jr. et al., 2002; Hague et al., 2020a; Hanifin et al., 2008) and snake lineages in two coevolutionary hotspots, California and the Pacific Northwest, convergently evolved escalated resistance via independent mutations in the pore region of the skeletal muscle voltage-gated sodium channel ($Na_V1.4$) that disrupt toxin binding (Geffeney et al., 2002, 2005; Hague et al., 2017). We examined whether cascading effects of the predator–prey arms race have led to the evolution of novel characters related to TTX resistance of snakes that retain prey toxins.

Newts are extremely toxic at some locations such as the central coast of Oregon (Hague et al., 2020a; Hanifin et al., 2008; Stokes et al., 2015), and as a result, TTX-resistant snakes can retain substantial amounts of TTX in their livers after consuming prey (Williams et al., 2004, 2012). TTX can persist in the liver for up to a month after consumption of a single newt, and at least 7 weeks after a steady diet of newts (i.e., 4–8 newts over a 5-week period). The retained levels of TTX are enough to kill a snake's own predators (Williams et al., 2004, 2012), which include mostly birds and some mammals (Ernst & Ernst, 2003; Rossman et al., 1996). Anecdotally, TTX-resistant snake populations that consume toxic newts also exhibit conspicuous colour patterns, especially along the Oregon coast (St. John, 2002; Stebbins, 2003). Most garter snakes are dull brown or black, but many western *Th. sirtalis* populations that are sympatric with toxic newts have bright red colour patterning on the dorsal body and head (Figure 1; St. John, 2002; Stebbins, 2003; Westphal, 2007), suggesting that TTX-resistant (and TTX-toxic) garter snakes have evolved a conspicuous warning signal to predators.

We sampled newt and garter snake populations across western North America to test whether the bright red coloration of snakes covaries clinally with newt TTX and snake resistance at the phenotypic interface of coevolution. Distinct TTX-resistant snake lineages in the California and Pacific Northwest hotspots (Figure S1; Hague

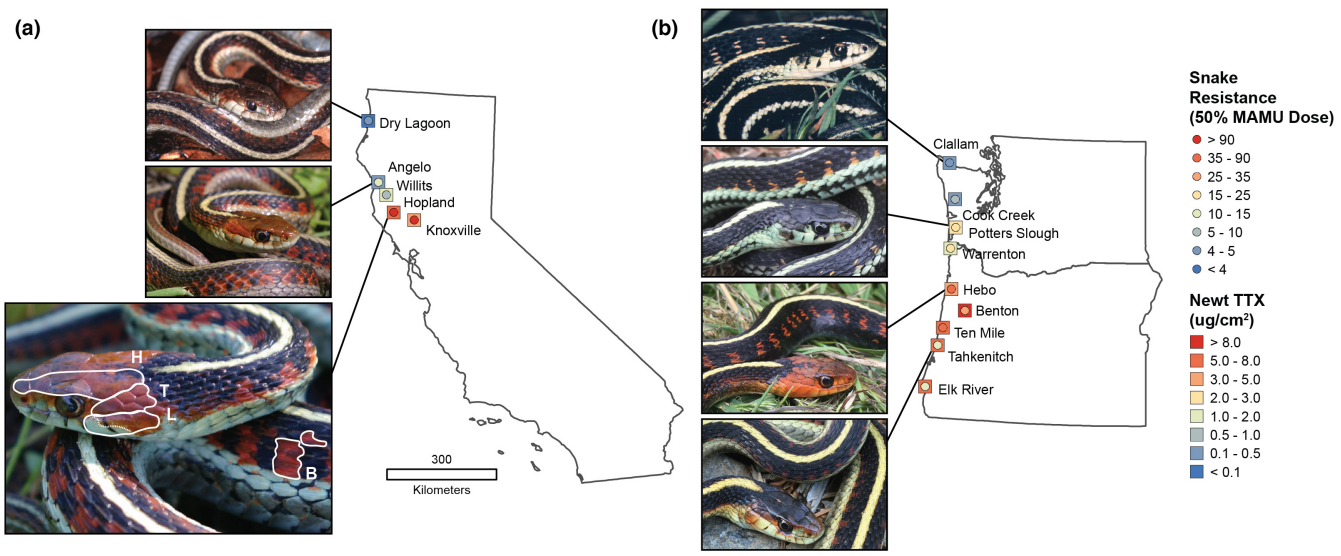

FIGURE 1 Latitudinal transects in (a) California and (b) the Pacific Northwest. To the right, the key indicates population estimates of garter snake phenotypic TTX resistance (50% MAMU dose, circles) and newt TTX (μg/cm^2, squares) along each transect. Representative images of snakes are show from different sampling localities. In (a), colour and area measurements are shown for snake dorsal blotches (b), major head scales (H), temporal scales (T), and labial scales (L). See Figure S1 for a phylogenetic analysis distinguishing the California and Pacific Northwest lineages.

et al., 2017) present two independent opportunities to test for relationships among newt TTX levels, snake resistance, and snake coloration. In the Pacific Northwest, we previously found that clines of snake phenotypic and genotypic TTX resistance tightly correlate with newt TTX levels and deviate from the neutral expectations of snake population genetic structure (Hague et al., 2020a). Here, we characterized a similar set of clines in California, and then, in both regions, measured red coloration (hue) and patterning on the dorsum and head of garter snakes. We used these data sets in California and the Pacific Northwest to test whether clines of escalating newt TTX and snake resistance are coincident with conspicuous red coloration on snakes.

2 | MATERIALS AND METHODS

We sampled prey and predator populations along two distinct transects: (1) five localities in northern California and (2) seven localities in the Pacific Northwest (Figure 1, Table S1). We leveraged our prior estimates from the Pacific Northwest of newt TTX levels, snake phenotypic and genotypic TTX resistance, and snake population genetic structure based on neutral SNPs (Hague et al., 2020a, 2020b) and used the same methods to generate similar data along the California transect (described below). We then analysed California and the Pacific Northwest separately as two distinct tests of snake colour variation, because *Th. sirtalis* in each region are genetically, geographically, and morphologically differentiated (Figure S1; Janzen et al., 2002; Hague et al., 2017, 2018), and the two lineages have independently evolved TTX resistance in response to toxic newts (Hague et al., 2017).

2.1 | TTX levels of newts

We first estimated newt TTX levels in California to measure the amount of defensive toxin at each locality along the transect. We quantified the amount of TTX in individual newts (N = 90 newts, Table S1) using a Competitive Inhibition Enzymatic Immunoassay (CIEIA) and TTX-specific antibodies (Gall et al., 2011; Stokes et al., 2012). We measured the amount of TTX in a 5 mm circular skin punch from the dorsum of each newt using a human skin-biopsy punch (Acu-Punche, Acuderm Inc.; Hague et al., 2016; Hanifin et al., 2002, 2004). These data were used to estimate the dorsal skin concentration of TTX ($\mu g/cm^2$) in each individual to account for differences in body size. TTX is uniformly distributed throughout the dorsum and levels of TTX in the dorsal skin are tightly correlated with levels in other regions (Hanifin et al., 2004). Distribution and leverage analyses indicated that a $x' = \log(x+0.1)$ transformation of TTX was needed. The transformed TTX values were used in the subsequent cline-fitting and correlation analyses along each transect (see below).

Multiple TTX-bearing newt species occur in central California and we found that rough-skinned newts (*Ta. granulosa*) and California newts (*Ta. torosa*) co-occur at two of our sampling localities in California, Willits and Knoxville (Table S1). We used a one-way ANOVA to test for species differences in TTX levels at Willits and Knoxville; however, we pooled the two species to generate mean TTX estimates of all newts at each locality for our downstream clinal analyses. There is no evidence that garter snakes preferentially prey on either species; although, snakes can self-assess resistance and behaviorally reject newts that are too toxic to ingest (Williams et al., 2003).

2.2 | Phenotypic TTX resistance of garter snakes

We estimated garter snake phenotypic TTX resistance at the five localities in California using a well-established assay of whole animal performance (Brodie III & Brodie Jr., 1990; Brodie Jr. et al., 2002; Hague et al., 2020a; Reimche et al., 2020; Ridenhour et al., 2004). Briefly, each snake was assayed on a 4 m racetrack to characterize its "baseline" crawl speed, then injected with a known dose of TTX and assayed for "post-injection" speed. Population estimates of TTX resistance are reported on a scale of mass-adjusted mouse units (MAMUs) to control for differences in body size (Brodie Jr. et al., 2002). Individuals from each locality received a series of TTX doses and resistance was estimated as the relative performance after injection: the MAMU dose of TTX that reduces performance by 50% of baseline speed. We found that nearly all of the snakes at Hopland and Knoxville were completely unaffected by our standard series of injections that range up to 250 MAMUs. Because most snakes were unaffected by our maximum dose, we were unable to estimate the population 50% MAMU doses and standard errors for these localities. We therefore assumed a minimum 50% dose of 250 MAMUs for these localities in subsequent analyses. We incorporated racetrack data from previous estimates of TTX resistance from the Dry Lagoon and Willits localities to generate more precise population estimates of TTX resistance for this study (N = 420 total snakes, Table S1; Brodie Jr. et al., 2002).

All statistics were performed in R 4.2.0 (R Core Team, 2022). The 50% MAMU dose was estimated separately for each locality from a dose–response curve using curvilinear regression and the general transform $y' = \ln(1/y - 1)$ (Brodie Jr. et al., 2002). At $y = 0.5$ (i.e., 50%), $y' = 0$ and the 50% dose is estimable $\hat{x} = -\alpha / \beta$ (where α is the intercept and β the slope from the curvilinear regression). Because $\hat{x}$ takes the form of a ratio, the standard error for the estimated 50% dose is calculated using standard methods for the variance of a ratio (Lynch & Walsh, 1998 p. 818; Brodie Jr. et al., 2002). Confidence intervals of 95% were calculated as ±1.96 SE. Regression was performed with the "lmer" function implemented in the lme4 package (Bates et al., 2015). The individual ID of each snake was included as a random effect to account for the fact that each snake received multiple injections. Distribution and leverage analysis indicated that a transformation of the x variable (MAMU of TTX) was needed, so we transformed the data using $x' = \ln(x+1)$ (Brodie Jr. et al., 2002). The transformed MAMU values were used in the subsequent cline-fitting and correlation analyses (see below).

2.3 | Genotypic TTX resistance of garter snakes

We also examined the frequency of snake TTX-resistance alleles in the skeletal muscle voltage-gated sodium channel ($Na_V1.4$). Garter snake lineages in California and the Pacific Northwest each independently evolved TTX resistance via mutations to the fourth domain pore-loop (DIV p-loop) of the $Na_V1.4$ channel (Geffeney et al., 2002, 2005; Hague et al., 2017). Snakes in both regions evolved an initial increase in TTX resistance via a repeated first-step I1561V mutation in the DIV p-loop (DIV^V) that disrupts toxin-binding at the pore. A second, highly resistant allele (DIV^{LVNV}) with three additional mutations (I1556L, D1568N, G1569V) is found exclusively in California, whereas a moderately resistant allele (DIV^{VA}) with one additional G1566A mutation is found exclusively in the Pacific Northwest (Hague et al., 2017). Importantly, the gene encoding $Na_V1.4$ (*SCN4A*) is located on the Z sex chromosome of *Th. sirtalis* (Gendreau et al., 2020). Colubrid snakes, including garter snakes, have heteromorphic sex chromosomes (ZZ males, ZW females), with recombination only occurring between Z chromosomes in males (Augstenová et al., 2018; Vicoso et al., 2013). Females are hemizygous for the Z-linked *SCN4A* gene, so allele frequency estimates must account for the fact that females have only one DIV p-loop allele. We previously estimated DIV allele frequencies at each locality using tissue samples from the snakes in this study (Gendreau et al., 2020; Hague et al., 2020a). These allele frequencies were used in the cline-fitting analyses (see below).

2.4 | Population genetic structure of snakes

We characterized the population genetic structure of snakes in California, which served as a neutral expectation of trait differentiation for snake TTX resistance and coloration (Hague et al., 2020a). We used double digest restriction-site associated DNA sequencing (ddRADseq) to generate a data set of neutral SNPs (Peterson et al., 2012), implementing the same methods we used previously to estimate snake population structure in the Pacific Northwest (Hague et al., 2020a). Briefly, genomic DNA was extracted using an DNeasy Blood & Tissue kit (Qiagen Inc.). We then digested 600 ng of genomic DNA from each sample using the restriction enzymes *MfeI* and *SbfI*. Unique combinations of individual P1 and P2 barcoded adapters were annealed to the digested genomic DNA of each sample. Samples were then pooled, purified with AmpureXP beads (Beckman Coulter, Inc.), and size selected for 500–600 bp fragments. The California samples were run with the (previously published) Pacific Northwest samples on two lanes of an Illumina HiSeq 2500 (Illumina, Inc.) to generate 125 bp paired-end reads.

We used *process_radtags* in Stacks 1.46 (Catchen et al., 2013) to demultiplex reads and remove sequences with low-quality scores or uncalled bases, producing an average of 1,715,216 reads per sample ($N = 86$ snakes). The reads were then aligned to the *Th. sirtalis* genome (Perry et al., 2018) using Bowtie2 2.2.9 (Langmead & Salzberg, 2012). We discarded reads that did not align or had more than one match to the genome. We then used *ref_map.pl* in Stacks to assemble the reference-aligned sequences into loci using a minimum depth (*–m*) of three, which produced an average of 10,605 loci per sample with a mean coverage of 84×.

We used *populations* in Stacks and the *dartR* package 2.0.4 in R (Gruber et al., 2017) to conduct additional filtering. In *populations*, we selected loci with a minimum depth of 10x coverage and retained one SNP per RAD locus to avoid linkage among sites. In *dartR*, we removed individuals with >30% missing data and removed loci with a minor allele frequency <5%. Finally, we used BayeScan 2.1 (Foll & Gaggiotti, 2008) to remove putative loci under selection. This analysis used 20 pilot runs with 5000 iterations followed by an additional burnin of 50,000 and then 50,000 output iterations. An outlier analysis with the FDR-corrected *p*-values (*q*-values) <.05 was used to identify and remove outlier loci putatively under selection. As a result, these additional filtering steps produced 635 neutral SNPs in 75 individuals that we used to assess population genetic structure in California. These loci were complemented by the 1027 neutral SNPs from 132 snakes that we previously generated from the Pacific Northwest (Hague et al., 2020a).

We generated summary statistics of population genetic diversity in California using the *hierfstat* package in R (Table S2; Goudet & Jombart, 2015) and evaluated population genetic differentiation by calculating global and pairwise F_{ST} values using the *hierfstat* and *stAMPP* R packages (Table S3; Pembleton et al., 2013). Finally, we summarized population genetic structure using a principal component analysis (PCA) using the "gl.pcoa" function in the *dartR* package (Figure S2). We retained the first and second axes from the PCA (capturing 9 and 5.1% of the variation, respectively) as a neutral expectation of population structure for our cline-fitting analyses (see below).

Finally, we used a subset of the filtered SNPs to conduct a phylogenetic analysis of western *Th. sirtalis*, which confirmed that populations in California and the Pacific Northwest represent two distinct lineages (Figure S1). We analysed our SNP data in a coalescent framework in the program SNAPP version 1.3.0 implemented in BEAST2 version 2.4.8 (Bouckaert et al., 2014; Bryant et al., 2012). Because SNAPP is computational intensive, we randomly selected a subset of 300 SNPs with no missing data that were present in both the California and Pacific Northwest data sets. The analysis included two individuals from each population, as well as two snakes sampled from Virginia as an outgroup. We estimated mutation rates (u and v) from the data sets and ran the MCMC for one million generations with the first 10% discarded as burnin. We checked for convergence using TRACER version 1.6 (Rambaut et al., 2014) and ensured that effective samples size (ESS) were > 200. TREEANNOTATOR (Bouckaert et al., 2014) was then used to find the maximum clade credibility tree and estimate posterior probabilities.

2.5 | Coloration of garter snakes

Next, in both California and the Pacific Northwest, we analysed snake colour and pattern variation on the dorsum and head, which

we expected to be the most obvious body regions to visually oriented predators such as birds (Figure 1 and Figure S3). We used a portable Perfection V19 colour scanner (Epson) to record images of garter snakes in the field along the California (N = 74 snakes) and Pacific Northwest (N = 88 snakes) transects. We imaged the same individual snakes that were used to collect the phenotypic and genomic data described above; however, we were unable to collect images at two of the nine Pacific Northwest localities, Warrenton and Benton, due to time constraints in the field. Live snakes were placed dorsum down on the scanner and pressed flat using a soft piece of foam to record images of the entire flattened dorsal body, including the head (Figure S3). Each image included a white balance and colour calibration chart (DGK colour tools) to account for minor variation in lighting in downstream analyses (but see below).

We used ImageJ 1.52 (Schneider et al., 2012) to quantify red coloration and patterning in four regions on the dorsal body and head: dorsal body blotches (B), major head scales (H), temporal scales (T), and labial scales (L) (Figure 1 and Figure S3). To measure each colour phenotype, we used the calibration chart to set the scale (mm) of the image and then used the "Freehand Selection" tool to trace a focal region of the snake and record red, green, blue (RGB) and area measurements (Figure S3). We used the calibration chart and the "CIPF chart white balance" function to control for slight differences in lighting between images when estimating RGB; however, colour-corrections did not alter the conclusions of our analyses, so only analyses of the unaltered images are presented herein. For each trait, we selected either the left or right side of the snake for measurements, depending on which side had the best image clarity.

First, we recorded RGB values and area measurements for red blotches along the dorsal body by selecting a representative region midbody and then outlining three consecutive dorsal blotches. We then divided the total area of the three patches by three to estimate the average blotch size for each snake. Because total blotch area depends on body size (Westphal et al., 2011), we regressed blotch area on snout-vent length (SVL) separately for the snakes from California and the Pacific Northwest. We then used the SVL-adjusted residual blotch area measurement in our analyses below along each transect. Second, we recorded RGB values for the major head scales, which included the parietal, supraocular, half of the frontal, prefrontal, and internasal scales (Rossman et al., 1996). Third, we measured RGB values for the temporal and post-temporal scales in the upper corner of the head. Fourth, we traced the red portion of the three upper labial scales at the corner of the mouth (usually scales 5–7) and recorded an RGB measurement. Here, we also measured the area of the red and non-red regions of the scales, which we used to calculate the proportion of total red area on the upper labial scales.

Finally, we used the "rgb2hsv" function in R to convert RGB values to hue, saturation, and value (HSV). Hue was used as a measure of pure colour (i.e., redness) of each region of the head and dorsum. In R, hue is represented by a continuous colour wheel ranging from 0 to 1, with pure red centered on 0, orange at values >0 (~0.1), and purple at values <1 (~0.9). To create a continuous set of hue values centered on red, we adjusted the colour wheel to range from 0.5 to 1.5, with pure red centered at 1, purple at hue values <1, and orange at values >1 (Figure 5). Lastly, we used one-way ANOVAs to test whether each colour trait varied among localities along each transect (Table S4). We used a nonparametric Kruskal-Wallis test (instead of an ANOVA) to evaluate population differences in the proportion of red on the labial scales of snakes. All snake colour traits varied significantly among localities along both transects, with the exception of temporal scales hue in the Pacific Northwest. We note that our estimates of hue on different parts of the snake dorsum and head are probably created by the same pigments (Westphal et al., 2011), and thus should not be interpreted as completely independent traits.

2.6 | Relating colour variation to newt TTX and snake resistance

We sought to test whether newt TTX and snake resistance levels along each transect covary with red coloration and patterning on snakes. We previously found in the Pacific Northwest that snake phenotypic and genotypic TTX resistance covary clinally with newt TTX levels, diverging from the neutral expectations of snake population genetic structure based on SNPs from ddRADseq (Hague et al., 2020a). We used this same cline analysis framework to test whether snake coloration and/or colour patterns covary clinally with arms race traits in California and the Pacific Northwest. We fit clines to (1) newt TTX levels, (2) snake phenotypic and genotypic TTX resistance, (3) the first two axes of variation from the PCA of neutral SNPs, and (4) snake colour traits. We then tested for concordance among the different clines by comparing the geographic center points of each cline function. To account for relationships that may not be encapsulated by the sigmoidal cline functions, we also tested for simple correlations among population means of the arms race traits and those of snake coloration and patterning; however, these results were generally consistent with the clinal analyses and the small number of localities limited our statistical power. Thus, the correlations are only reported in Figures S4–S7, Table S5.

We used the *HZAR* package in R (Derryberry et al., 2014) to fit maximum likelihood clines along each transect. We calculated distances along each cline as kilometres (km) from the northernmost sampling sites: Dry Lagoon in California and Clallam in the Pacific Northwest. We used the "hzar.doNormalData1DPops" function and the mean and variance of each trait to fit separate clines for each of the arms race traits and colour phenotypes. The two locations in California (Hopland and Knoxville) with extreme levels of snake phenotypic TTX resistance that exceeded our assay were assigned a MAMU dose of 250 and a variance of 0. We used the "hzar.doNormalData1Draw" function to fit clines to the individual PC1 and PC2 values from the PCA of neutral SNPs representing snake population genetic structure. Here, we focused visually on the first axis of variation (PC1), because it tended to capture latitudinal population structure in both California and the Pacific Northwest; however, the full results are shown in Table 1. For

TABLE 1 Results from cline-fitting analyses. Mean trait values, their geographic centre points along the cline, and cline widths are shown for each transect, along with confidence intervals (CIs). Clines were fit to snake TTX-resistance alleles using the frequency of TTX-resistance alleles in the DIV p-loop of $Na_V1.4$ in California (DIV^{LVNV}) and the Pacific Northwest (DIV^{V} and DIV^{VA})

	California						Pacific Northwest					
Trait	Mean	Center (km)	Lower CI	Upper CI	Width (km)	Lower CI	Upper CI	Mean	Center (km)	Lower CI	Upper CI	Width (km)	Lower CI	Upper CI
Newt TTX	−0.028	197.670	191.771	225.579	148.580	146.270	238.074	0.118	193.184	168.778	200.283	284.949	207.732	363.750
Snake Phenotypic TTX Resistance	3.614	217.610	211.505	229.465	20.517	6.231	42.230	2.350	128.543	113.922	173.242	510.820	314.218	539.450
Snake Genotypic TTX Resistance	0.464	213.588	209.395	232.475	10.763	1.204	44.844	0.500	128.843	104.118	149.925	55.589	5.569	101.699
Neutral PC1	−0.841	129.287	20.089	152.228	125.932	72.117	287.401	1.119	438.199	414.155	479.387	497.404	401.353	610.354
Neutral PC2	−0.921	274.102	261.646	295.679	0.029	0.009	23.517	−0.667	500.256	493.574	553.979	33.565	11.499	127.700
Dorsal Blotches Hue	1.011	250.714	216.013	252.848	6.827	3.027	29.091	1.022	125.897	49.853	125.897	475.568	391.116	532.783
Dorsal Blotches Area (SVL-adjusted)	−0.467	230.452	194.968	256.602	7.157	0.022	65.899	−0.340	229.983	179.408	329.120	54.831	0.288	183.732
Major Head Scales Hue	1.007	123.644	3.974	157.783	12.361	0.112	57.104	0.982	170.907	139.316	233.237	156.436	47.470	201.291
Temporal Scales Hue	1.015	228.403	174.175	234.893	16.934	0.048	37.200	1.013	184.518	152.741	222.748	71.372	9.280	102.815
Labial Scales Hue	1.039	259.671	258.812	294.371	52.250	44.111	131.928	1.029	196.208	159.153	246.024	36.196	10.161	101.268
Labial Scales Proportion Red	0.296	185.352	183.355	204.347	11.723	0.924	11.723	0.259	383.597	342.882	398.696	76.185	39.955	140.092

each of the data sets described above, we ran five separate models that varied in the number of cline shape parameters estimated. All models estimated the cline center (distance from sampling location 1, *c*) and width (1/maximum slope, *w*), but could additionally estimate combinations of exponential decay curve (tail) parameters (neither tail, right tail only, left tail only, mirrored tails, or both tails separately), which represent the distance from the cline centre to the tail (δ) and the slope of the tail (τ). Lastly, we used the "hzar.doMolecularData1DPops" to fit clines to the frequency of TTX-resistance alleles in snake populations. In addition to the cline shape parameters listed above, the genetic models also varied as to whether they estimated allele frequencies at the cline ends (p_{min} and p_{max}) or fixed them at 0 and 1.

For each trait, we compared the different models using AIC corrected for small sample sizes (AICc) and extracted maximum likelihood parameters for the best-fitting model. We considered geographic cline centres with nonoverlapping two log-likelihood unit support limits (confidence intervals; CIs) to occur in significantly different geographic locations (Baldassarre et al., 2014; Hague et al., 2020a; Scordato et al., 2017). All results presented herein are newly reported with the exception of the previously estimated clines from the Pacific Northwest on newt TTX, snake phenotypic and genotypic TTX resistance, and snake population structure (Hague et al., 2020a).

3 | RESULTS

3.1 | Replicate clines of prey toxicity and predator resistance

We first measured newt TTX in California to gauge levels of defensive toxin at each site. TTX levels were quite variable among the California localities (one-way ANOVA, $F_{(4,85)} = 27.7$, $p < .001$), reaching high levels at the southern end of the transect (Figure 2). The newt species *Ta. torosa* had significantly higher TTX than *Ta. granulosa* at Knoxville ($F_{(1,35)} = 170.6$, $p < .001$), but not at Willits ($F_{(1,13)} = 4.5$, $p = .053$), although the trend was in the same direction. These escalating levels of newt TTX were accompanied by sharp increases in snake phenotypic and genotypic TTX resistance along the transect. We found low levels of resistance in northern populations, increasing to extreme levels of TTX resistance (>250 MAMUs) at the southern Hopland and Knoxville localities, where we also found a high frequency of the highly resistant DIV^{LVNV} allele in the $Na_V1.4$ channel (Figure 2).

Our clinal analyses revealed that snake TTX resistance was tightly correlated with newt TTX along the California transect, as indicated by coincident clines of predator resistance and prey toxins (Figures 4 and 5). The geographic centre points for clines of snake phenotypic and genotypic TTX resistance were located within 4 km of each other and did not differ statistically from the cline centre point of newt TTX (Table 1). All three cline centre points fell within only 19.9 km of each other along the 298 km California transect.

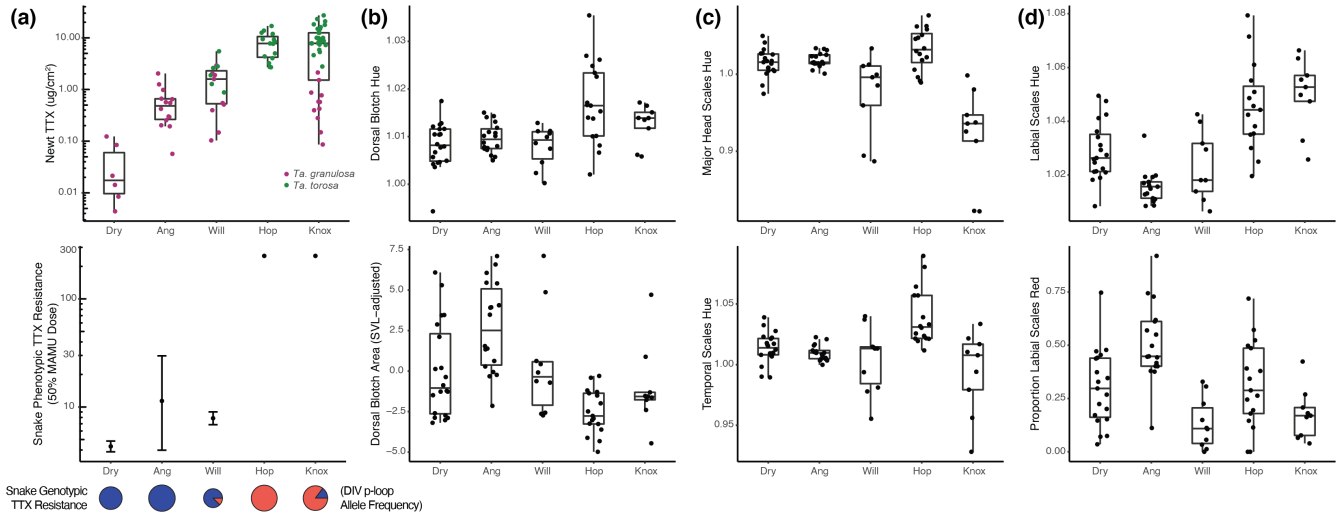

FIGURE 2 Trait variation along the California transect in (a) arms race traits (newt TTX and snake TTX resistance), (b) snake dorsal blotch colour and size, (c) head scale colour, and (d) labial scale colour. Boxplots show medians, first and third quartiles (hinges), and the smallest/largest values within 1.5*IQR of the hinges (whiskers). For newt TTX, individual points are colour-coded by newt species. For snake phenotypic TTX resistance, points indicate 50% MAMU doses with error bars representing 95% confidence intervals. TTX resistance at Hopland (Hop) and Knoxville (Knox) is shown as a minimum of 250 MAMUs, because we were unable to generate 50% dose estimates due to extreme levels of TTX resistance. Observed frequencies of snake TTX-resistance alleles found in California are shown as pie charts below the phenotypic estimates. The ancestral allele of the $Na_V1.4$ DIV p-loop (DIV^+) is shown in dark blue, along with the highly resistant DIV^{LVNV} allele in pink. Pie chart size is proportional to sample size.

The snake resistance clines showed a clear signature of adaptation to local toxin levels of newts, diverging from the expectations of snake population genetic structure based on the neutral SNPs. F_{ST} values from the SNP data were moderate (global $F_{ST} = 0.097$, 95% CI [0.09, 0.105]; Table S3) and the primary axis of variation from the PCA (PC1) captured latitudinal differentiation between the northernmost site Dry Lagoon and the southern localities (Figure S2). The geographic centre point of the PC1 cline representing population structure was located a distant 88.3 km away from that of the phenotypic TTX resistance cline. Similarly, the PC2 cline did not align with TTX resistance (Table 1). This pattern where clinal variation of snake resistance diverges from neutral expectations and tracks newt TTX levels is very similar to our previous findings in the Pacific Northwest, where the cline centre points of snake phenotypic and genotypic resistance and newt TTX were all located within 64.6 km of each other along the 611 km transect (Figures 3–5, Table 1; Hague et al., 2020a).

3.2 | Concordance of snake coloration with coevolutionary traits

Our cline-fitting analysis revealed that clines of snake coloration overlapped substantially with the coevolutionary clines along both transects, while also deviating from the neutral expectations of snake population genetic structure (Figures 4 and 5). Snake coloration in the Pacific Northwest exhibited the most intuitive pattern of conspicuous coloration. Here, the geographic centre points of clines representing dorsal blotch hue, dorsal blotch size, major head scales hue, temporal scales hue, and labial scales hue all overlapped with the cline centres of newt TTX, snake phenotypic TTX resistance, and/or genotypic TTX resistance (Figure 4, Table 1). Lower hue values (reddish-purple) for the colour phenotypes on the dorsum and head were generally associated with increasing levels of newt TTX and snake resistance along the cline. Visual inspection revealed that dorsal blotch hue and area exhibited the clearest patterns of clinal concordance with coevolutionary traits (Figure 5). Mean dorsal blotch area also had a strong positive correlation with newt TTX levels ($r_{(5)} = 0.757$, $p = .049$) and snake phenotypic resistance ($r_{(5)} = 0.666$, $p = .103$; Figure S5, Table S5), although our correlational analyses were generally underpowered (Figure S7). This positive relationship of dorsal blotch area with newt TTX and snake resistance is consistent with the hypothesis that TTX-resistant garter snakes in central Oregon that can retain large amounts of newt TTX have also evolved a conspicuous red colour pattern.

Many of the snake colour clines in California also had geographic center points that overlap with those of the arms race; however, the overall pattern was less intuitive than the Pacific Northwest. The geographic centre points for dorsal blotch hue, dorsal blotch area, temporal scales hue, and the proportion of labial scales with red all overlapped with the centre points of newt TTX levels, snake phenotypic TTX resistance, and/or genotypic TTX resistance in California (Figure 4). Higher hue values (reddish-orange) for the colour traits were generally associated with increasing levels of newt TTX and snake resistance along the cline, which was opposite the pattern we observed in the Pacific Northwest. Visual inspection indicated that dorsal blotch hue, dorsal blotch area, and the proportion of red on labial scales varied clinally with the coevolutionary traits and departed from expectations of snake population structure (Figure 5). Mean dorsal

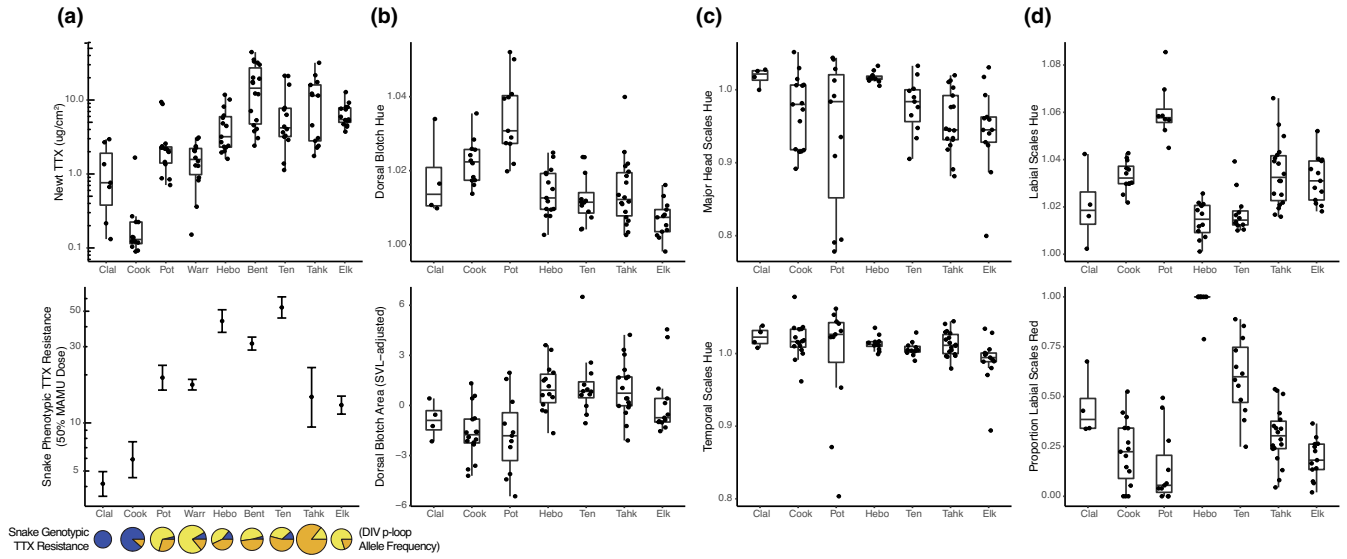

FIGURE 3 Trait variation along the Pacific Northwest transect in (a) arms race traits (newt TTX and snake TTX resistance), (b) snake dorsal blotch colour and size, (c) head scale colour, and (d) labial scale colour. Estimates of newt TTX and snake TTX resistance are from Hague et al. (2020a, 2020b). Observed frequencies of snake TTX-resistance alleles found in the Pacific Northwest are shown as pie charts below the phenotypic estimates. The ancestral allele of the $Na_V1.4$ DIV p-loop (DIV^+) is shown in dark blue, along with TTX-resistance alleles of increasing resistance (DIV^V, light yellow; DIV^{VA}, orange). Pie chart size is proportional to sample size.

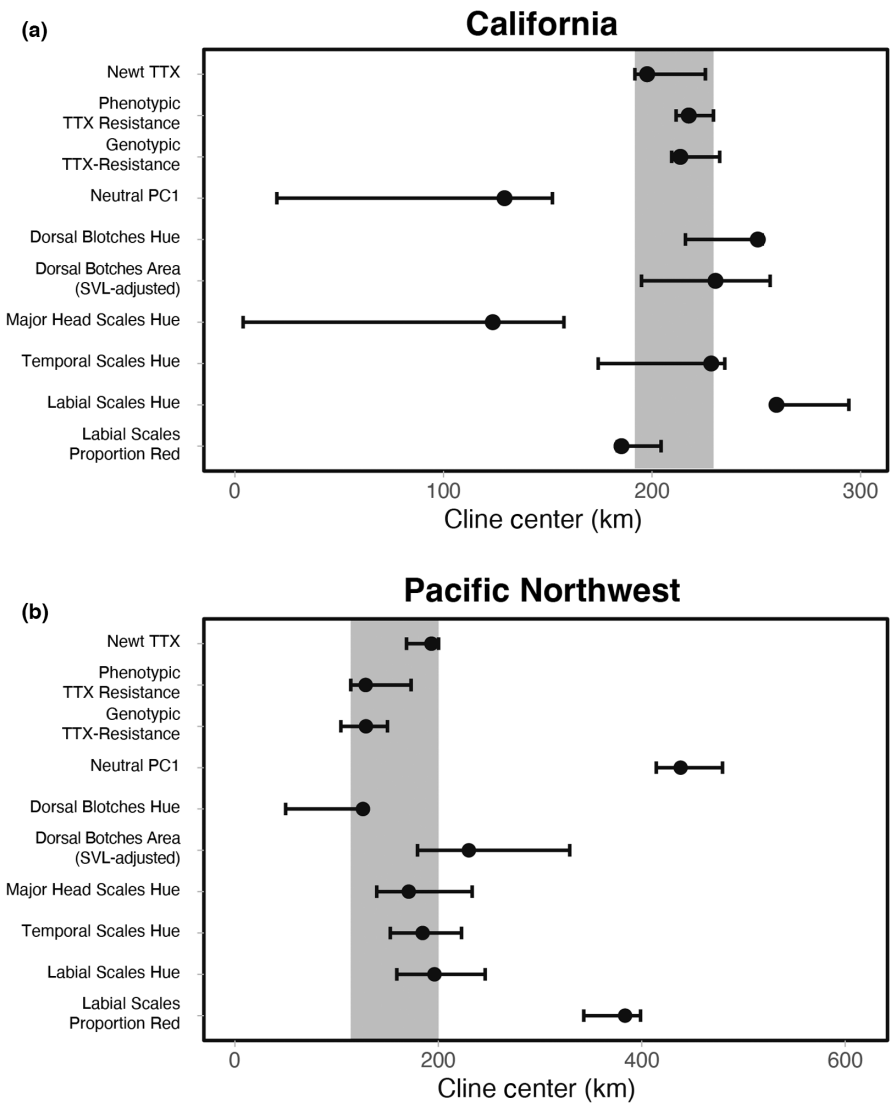

FIGURE 4 Geographic centre points for clines in (a) California and (b) the Pacific Northwest. Error bars indicate confidence intervals (CIs) surrounding the geographic centre point of each cline. The vertical grey bands highlight the geographic distance between the cline centre points for newt TTX and snake phenotypic resistance (±95% CIs).

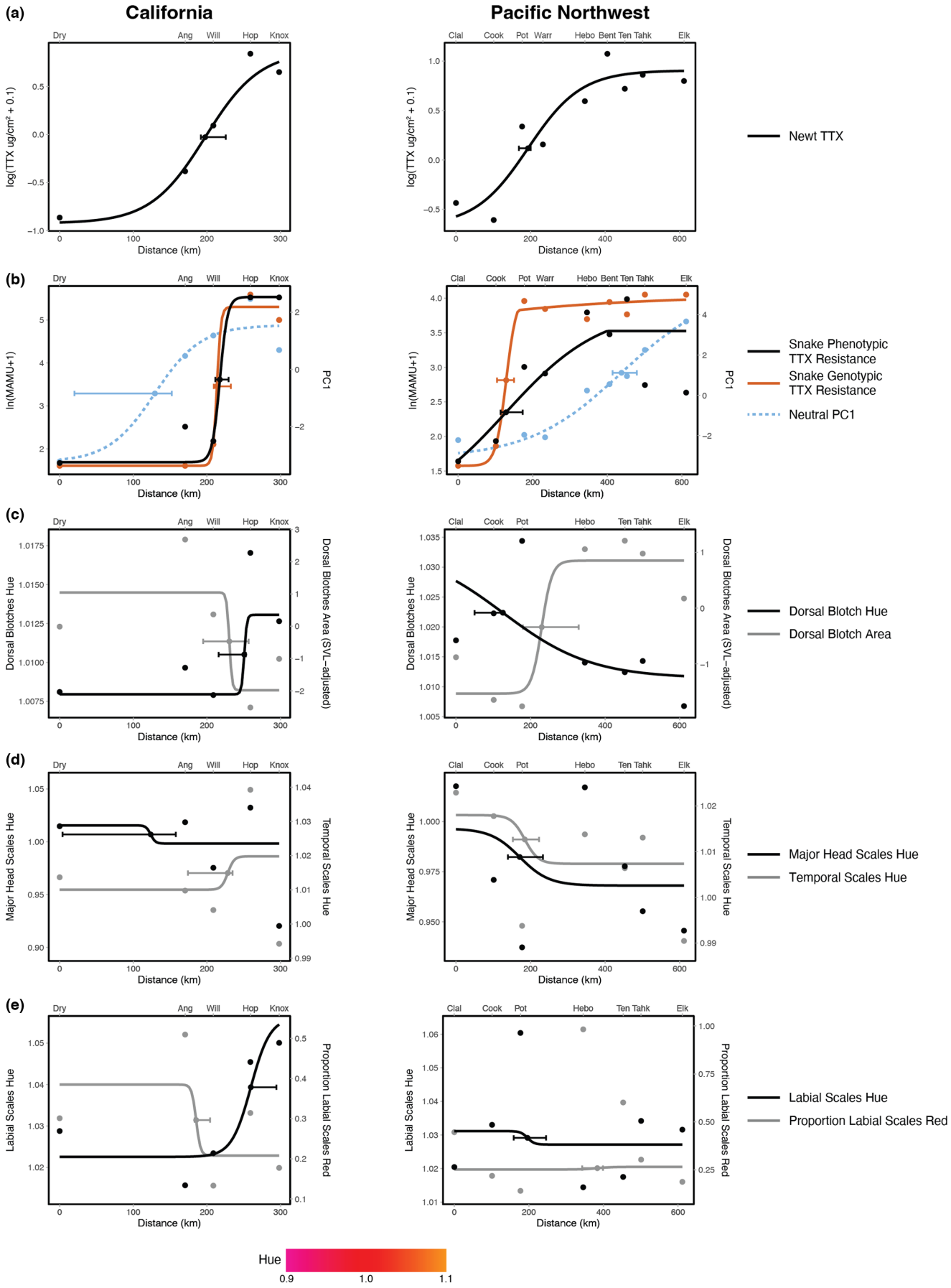

FIGURE 5 Legend on next page

FIGURE 5 Clinal analyses in California and the Pacific Northwest of (a) newt TTX levels, (b) snake TTX resistance and population structure, (c) snake dorsal blotches, (d) head scales, and (e) labial scales. Error bars indicate confidence intervals (CIs) surrounding the geographic centre point of each cline. Below, hue values are shown ranging from purplish-red (0.9) to red (1.0) to orangish-red (1.1), with saturation and value held constant at 100%.

blotch hue also had a strong correlation with the coevolutionary traits, such that mean hue was positively correlated with newt TTX levels ($r_{(3)} = 0.813$, $p = .094$) and snake phenotypic resistance ($r_{(3)} = 0.906$, $p = .034$; Figure S4, Table S5). Notably, colour pattern variation in California generally ran counter to our observations in the Pacific Northwest. Increasing levels of newt TTX and snake resistance along the California cline were associated with declining dorsal blotch area and a declining proportion of red on labial scales.

4 | DISCUSSION

We found that garter snake coloration deviates from neutral expectations and covaries with escalating newt TTX and snake resistance along replicate clines in California and the Pacific Northwest (Figures 4 and 5), supporting anecdotal observations that coloration has evolved in conjunction with hotspots of snake-newt coevolution at the phenotypic interface. However, the two snake lineages exhibited different patterns of a putative warning signal. Below, we discuss evidence that snake coloration has evolved in concert with the arms race in the geographic mosaic of coevolution, and evaluate how cascading effects of coevolution may potentially implicate other levels of trophic interaction.

The relationship between snake coloration and coevolutionary traits exhibited clear differences in the Pacific Northwest and California. In the Pacific Northwest, red dorsal blotches increase in size and decrease in hue value (trending towards reddish-purple) as newt TTX and snake resistance escalate at the southern end of the cline in central/southern Oregon (Figure 5). This pattern contrasted the direction in California, where dorsal blotches tended to decrease in size and increase in hue value (towards reddish-orange) with arms race escalation at the southern end of the transect. The proportion of red on labial scales also declined with coevolutionary traits in California. Despite these differences between the Pacific Northwest and California, we note that TTX-resistant snakes in each region did exhibit some colour similarities, as highly resistant snakes at the southern end of each transect converged on roughly similar dorsal blotch hue values of ~1.015 (Figure 5). Importantly, these clines of snake coloration in both regions deviate from the major axes of variation from the PCAs of neutral SNPs (Table 1), implying that colour variation is not simply a consequence of snake population genetic structure.

At least in the Pacific Northwest, the concordant clines of snake dorsal blotch size/colour, newt TTX, and snake resistance are consistent with the hypothesis that garter snakes exhibit conspicuous red colours as a warning to potential predators in hotspots where TTX-resistant snakes consume toxic newts. Bright red coloration is a common element in aposematic signalling, especially for signalling to avian predators (Brodie Jr., 1977; Gamberale-Stille & Guilford, 2003; Mochida, 2009; Roper, 1990). Although we do not know how predators might perceive observed variation in red hue, the relatively large dorsal blotches on TTX-resistant snakes in central Oregon are consistent with an aposematic trait. Moreover, newts in central and southern Oregon, particularly Benton County, are the most toxic known *Taricha* populations in western North America (Figure 1; Hague et al., 2020a; Hanifin et al., 2008; Stokes et al., 2015; Williams et al., 2004). The ability of garter snakes to retain TTX in their livers was originally discovered in central Oregon (Williams et al., 2004), where we also observed the bright red coloration on snakes that helped motivate this study.

The conspicuousness of red coloration on the dorsal blotches suggests they may serve as a warning signal. When confronted by predators, garter snakes normally expose a startle coloration by expanding their bodies to reveal the white (ancestral) or red (derived in *Th. sirtalis*) hidden in the integument between dorsal scales (Cott, 1940; Shine et al., 2000; Westphal & Morgan, 2010). However, the red dorsal blotches on *Th. sirtalis* in western North America are also present on the surface of dorsal scales (Figure 1), making the blotches constantly visible and conspicuous. Crypsis-violating patterns such as these are generally only expected to evolve in snakes with a toxic or venomous defence, or snakes with a sympatric model that is toxic/venomous (but see below; Westphal, 2007).

The different patterns we observed in the Pacific Northwest versus California could be explained by a number of factors. Due to field constraints, our transect in California did not include southern localities along the central coast, including in the Bay Area, where TTX-toxic newts and highly resistant snakes have been found in the past (Brodie Jr. et al., 2002; Feldman et al., 2010; Hanifin et al., 2008). These populations include the federally endangered subspecies *Th. sirtalis tetrataenia*, which is described as one of the most visually striking snakes in North America with a vibrant red head and bright red dorsolateral stripes (Stebbins, 2003). Further south, newts contain less TTX and *Th. sirtalis* are less resistant (Brodie Jr. et al., 2002; Hanifin et al., 2008), which seems to coincide with a reduction in red coloration on the head and along the body (Stebbins, 2003). These southern localities may help elucidate the relationships among newt TTX, snake resistance, and snake coloration in California.

Garter snakes in California and the Pacific Northwest also interact with different newt species. *Taricha granulosa* is the only TTX-bearing newt species in the Pacific Northwest, whereas two additional species, *Ta. torosa* and *Ta. rivulosa*, are found in California. TTX levels can also differ among newt species in California (Hanifin et al., 2008), even within a single location. For instance, we found that *Ta. granulosa* has significantly lower levels of TTX than *Ta. torosa* at the Knoxville locality ($p < .001$). There is no evidence that

garter snakes preferentially prey on either *Taricha* species, so prey could contain quite variable levels of TTX at sites like Knoxville. If prey are not consistently toxic enough for snakes to retain large quantities of TTX, then conspicuous warning coloration may not be strongly favoured in California populations with multiple newt species.

Finally, garter snakes in California and the Pacific Northwest are geographically and genetically differentiated (Figure S1; Janzen et al., 2002; Hague et al., 2017, Hague et al., 2020a), and as a result, these lineages have experienced different evolutionary histories and selective pressures that probably influenced colour variation in complex, unknown ways. For instance, there could be unmeasured aspects of snake coloration or other characters in California that influence predator responses in ways we do not understand. In the future, inferences of aposematism will be aided by documenting predator communities in California and the Pacific Northwest, as well as the colour perception of dominant predators in each region (Endler & Mielke Jr., 2005; Maia et al., 2013).

The contrasting nature of our results in the Pacific Northwest and California motivates consideration of other explanations for why clines of snake coloration might exist. Population differences in snake colour and pattern may be due to variation in light environments, which could influence colour perception by predators (Endler, 1993). For example, red colours could aid with crypsis (rather than conspicuousness) in certain local environments. Garter snakes often inhabit thickets of willow and brambles of blackberry or other shrubs with bright red and yellow leaves and stems, especially in autumn. An irregular red blotched pattern on the dorsum could have a cryptic function that minimizes initial detection by predators (Allen et al., 2013; Brodie III, 1989, 1992; Jackson et al., 1976). A similar crypsis hypothesis has been proposed for the red dorsal stripe on *Plethodon cinereus* salamanders, which may help individuals blend in with reddish leaf litter on the forest floor (Venesky & Anthony, 2007). Moving forward, explicit tests of predator responses (e.g., with plasticine models) could illuminate the cryptic or aposematic functions of these colour pattern elements (Brodie III, 1993; Brodie III & Janzen, 1995; Pfennig & Mullen, 2010). It is unlikely that dorsal coloration is under sexual selection, because courtship of *Th. sirtalis* is primarily mediated by olfactory signals (Mason et al., 1989; Mason & Parker, 2010; Westphal, 2007), with no evidence that visual signals are involved.

Interestingly, red dorsolateral coloration has evolved independently in two other western *Thamnophis* species, *Th. elegans* and *Th. ordinoides*, that co-occur with *Taricha* (Figure 6; St. John, 2002; Westphal, 2007). In particular, *Th. elegans* in central coastal California can bear striking resemblance to local *Th. sirtalis*, with red dorsal coloration organized into recognizable blotches (St. John, 2002; Stebbins, 2003). However, both *Th. elegans* and *Th. ordinoides* are sensitive to TTX (Feldman et al., 2009, 2020; Motychak et al., 1999), and are unlikely to consume newts and sequester TTX like *Th. sirtalis* (Westphal, 2007; Williams et al., 2004). The red dorsal coloration on *Th. elegans* could be a form of Batesian mimicry to TTX-toxic *Th. sirtalis* in sympatric populations with highly toxic newts (E.D. Brodie III personal observation; Westphal, 2007). Alternatively, the presence of red coloration on three *Thamnophis* species that share roughly similar habitats could be due to similar selective pressures, for example, for crypsis in relation to similar backgrounds (e.g., Sweet, 1985). Two other western *Thamnophis* species, *Th. couchii* and *Th. atratus*, have evolved escalated TTX resistance in response to toxic newts (Feldman et al., 2009, 2010), although it remains unknown whether these species sequester TTX. *Th. couchii* lacks any red coloration; however, highly resistant *Th. atratus* can be found with a bright orangish-red dorsal stripe in central coastal California where toxic newts occur (Rossman et al., 1996; Stebbins, 2003).

In summary, we find evidence that snake coloration covaries with clinal escalation of newt TTX and snake resistance surrounding two hotspots in the geographic mosaic of arms race coevolution. In the Pacific Northwest, clinal increases in red dorsal blotches match predictions of an aposematic warning signal, suggesting that cascading effects of the arms race have led to a novel trait in resistant predators that retain prey toxins. Interactions between toxic prey and resistant predators seem especially likely to generate effects that extend to other trophic levels. For example, snakes in the related Natricine genus *Rhabodophis* sequester defensive bufadienolide toxins from toad and firefly prey and also display red patches on interscalar tissue when threatened (Fukuda et al., 2021; Hutchinson et al., 2007, 2012; Mori et al., 2012; Yoshida et al., 2020). Similarly, toxin-resistant monarch butterflies sequester the defensive cardiac glycosides in milkweeds and, as a result, some of the butterflies' avian and mammalian predators seem to have also evolved toxin-resistant mutations (Groen & Whiteman, 2021; Karageorgi et al., 2019; Petschenka & Agrawal, 2015).

FIGURE 6 *Thamnophis* species found in western North America that display conspicuous red coloration and co-occur with TTX-bearing *Taricha* newts. (a) *Th. sirtalis* (photo from Hopland, CA), (b) *Th. elegans* (San Mateo, CA; credit R.W. Hansen), and (c) *Th. ordinoides* (Hebo, OR).

Together, these studies illustrate how coevolution at the phenotypic interface of a two-species arms race can become an indirect gateway to evolutionary innovation along unrelated phenotypic axes. In the case of garter snakes, coevolution with newts seems to have indirectly led to the evolution of a novel aposematic trait that has no bearing on outcomes in the pairwise arms race itself. Innovations like these can cascade to additional trophic interactions (e.g., avian predators), because coevolving species exist within a much larger network of interacting species (Andreazzi et al., 2017; Guimarães et al., 2017). In the geographic mosaic of coevolution, hotspots represent locations on the landscape where two focal species experience intense reciprocal selection (Thompson, 1999, 2005). Our findings here suggest that these locations could also represent hotspots of evolutionary innovation that cascade to interactions with other local species.

AUTHOR CONTRIBUTIONS

Michael T. J. Hague and Edmund D. Brodie III conceived the project. Michael T. J. Hague collected specimens, generated genetic data, and performed statistical analyses. Lauren E. Miller collected and analysed coloration data. Amber N. Stokes collected newt TTX data. Chris R. Feldman and Edmund D. Brodie Jr. collected data on snake phenotypic TTX resistance. Edmund D. Brodie III coordinated the project and provided leadership. Michael T. J. Hague and Edmund D. Brodie III edited the manuscript, with input from the other authors.

ACKNOWLEDGEMENTS

We thank the Departments of Fish and Wildlife in California, Oregon, and Washington for scientific collecting permits to MTJH (CA: SC-11937, OR: 063-18, and WA: 18-082). We also thank USU and UNR IACUC for protocols to EDB Jr. and CRF, and H. Moniz and G. Blaustein for aid with live animals. We are grateful for the staff and resources at the Hopland Research and Extension centre, the UC Natural Reserve System, and Sonoma Mountain Ranch (J. Wilcox). We are especially thankful for T. St. Pierre's help with fieldwork. S. Brodie first suggested the possibility that *Th. elegans* might be mimicking *Th. sirtalis* in some areas while helping with fieldwork. This study was supported by NSF DEB 1601296 to MTJH and EDB III, NSF IOS 1355221 to CRF, and NSF DEB 1911485 to EDB III.

CONFLICT OF INTEREST

The authors declare no conflict of interest.

DATA AVAILABILITY STATEMENT

Newly reported phenotypic and genetic data and scripts have been made available on Dryad at https://doi.org/10.5061/dryad.d7wm37q4n. Previously published data from the Pacific Northwest are available at https://doi.org/10.5061/dryad.51c59zw5k.

ORCID

Michael T. J. Hague https://orcid.org/0000-0003-0641-2420
Amber N. Stokes https://orcid.org/0000-0001-6935-7794
Chris R. Feldman https://orcid.org/0000-0003-2988-3145
Edmund D. Brodie Jr https://orcid.org/0000-0002-5739-4747
Edmund D. Brodie III https://orcid.org/0000-0001-9231-8347

REFERENCES

Allen, W. L., Baddeley, R., Scott-Samuel, N. E., & Cuthill, I. C. (2013). The evolution and function of pattern diversity in snakes. *Behavioral Ecology*, *24*, 1237–1250.

Andreazzi, C. S., Thompson, J. N., & Guimaraes, P. R., Jr. (2017). Network structure and selection asymmetry drive coevolution in species-rich antagonistic interactions. *The American Naturalist*, *190*, 99–115.

Augstenová, B., Johnson Pokorná, M., Altmanová, M., Frynta, D., Rovatsos, M., & Kratochvíl, L. (2018). ZW, XY, and yet ZW: Sex chromosome evolution in snakes even more complicated. *Evolution*, *72*, 1701–1707.

Baldassarre, D. T., White, T. A., Karubian, J., & Webster, M. S. (2014). Genomic and morphological analysis of a semipermeable avian hybrid zone suggests asymmetrical introgression of a sexual signal. *Evolution*, *68*, 2644–2657.

Bates, D., Mächler, M., Bolker, B., & Walker, S. (2015). Fitting linear mixed-effects models using lme4. *Journal of Statistical Software*, *67*, 1–48.

Benkman, C. W., Parchman, T. L., Favis, A., & Siepielski, A. M. (2003). Reciprocal selection causes a coevolutionary arms race between crossbills and lodgepole pine. *The American Naturalist*, *162*, 182–194.

Bouckaert, R., Heled, J., Kühnert, D., Vaughan, T., Wu, C.-H., Xie, D., Suchard, M. A., Rambaut, A., & Drummond, A. J. (2014). BEAST 2: A software platform for Bayesian evolutionary analysis. *PLoS Computational Biology*, *10*, e1003537.

Brodie, E. D., III. (1989). Genetic correlations between morphology and antipredator behaviour in natural populations of the garter snake *Thamnophis ordinoides*. *Nature*, *342*, 542–543.

Brodie, E. D., III. (1992). Correlational selection for color pattern and antipredator behavior in the garter snake *Thamnophis ordinoides*. *Evolution*, *46*, 1284–1298.

Brodie, E. D., III. (1993). Differential avoidance of coral snake banded patterns by free-ranging avian predators in Costa Rica. *Evolution*, *47*, 227–235.

Brodie, E. D., III, & Brodie, E. D., Jr. (1990). Tetrodotoxin resistance in garter snakes: An evolutionary response of predators to dangerous prey. *Evolution*, *44*, 651–659.

Brodie, E. D., III, & Brodie, E. D., Jr. (1999). Predator-prey arms races. *Bioscience*, *49*, 557–568.

Brodie, E. D., III, & Janzen, F. (1995). Experimental studies of coral snake mimicry: Generalized avoidance of ringed snake patterns by free-ranging avian predators. *Functional Ecology*, *9*, 186–190.

Brodie, E. D., III, & Ridenhour, B. J. (2003). Reciprocal selection at the phenotypic interface of coevolution. *Integrative and Comparative Biology*, *43*, 408–418.

Brodie, E. D., Jr. (1977). Salamander antipredator postures. *Copeia*, *1977*, 523–535.

Brodie, E. D., Jr., Ridenhour, B. J., & Brodie, E. D., III. (2002). The evolutionary response of predators to dangerous prey: Hotspots and coldspots in the geographic mosaic of coevolution between garter snakes and newts. *Evolution*, *56*, 2067–2082.

Bryant, D., Bouckaert, R., Felsenstein, J., Rosenberg, N. A., & RoyChoudhury, A. (2012). Inferring species trees directly from biallelic genetic markers: Bypassing gene trees in a full coalescent analysis. *Molecular Biology and Evolution*, *29*, 1917–1932.

Catchen, J., Bassham, S., Wilson, T., Currey, M., O'Brien, C., Yeates, Q., & Cresko, W. A. (2013). The population structure and recent colonization history of Oregon threespine stickleback determined using restriction-site associated DNA-sequencing. *Molecular Ecology*, *22*, 2864–2883.

Cott, H. B. (1940). *Adaptive coloration in animals*. Methuen & Co. Ltd.

Dawkins, R., & Krebs, J. R. (1979). Arms races between and within species. *Proceedings of the Royal Society of London - Series B: Biological Sciences*, *205*, 489–511.

Derryberry, E. P., Derryberry, G. E., Maley, J. M., & Brumfield, R. T. (2014). HZAR: Hybrid zone analysis using an R software package. *Molecular Ecology Resources*, *14*, 652–663.

Dobler, S., Dalla, S., Wagschal, V., & Agrawal, A. A. (2012). Community-wide convergent evolution in insect adaptation to toxic cardenolides by substitutions in the Na, K-ATPase. *Proceedings of the National Academy of Sciences of the United States of America*, *109*, 13040–13045.

Ehrlich, P. R., & Raven, P. H. (1964). Butterflies and plants: A study in coevolution. *Evolution*, *18*, 586–608.

Endler, J. A. (1993). The color of light in forests and its implications. *Ecological Monographs*, *63*, 1–27.

Endler, J. A., & Mielke, P. W., Jr. (2005). Comparing entire colour patterns as birds see them. *Biological Journal of the Linnean Society*, *86*, 405–431.

Ernst, C. H., & Ernst, E. M. (2003). *Snakes of the United States and Canada*. Smithsonian Books.

Feldman, C., Hansen, R., & Sikola, R. (2020). *Thamnophis elegans*. Tetrodotoxin poisoning. *Herpetological Review*, *51*, 630–631.

Feldman, C. R., Brodie, E. D., Jr., Brodie, E. D., III, & Pfrender, M. E. (2009). The evolutionary origins of beneficial alleles during the repeated adaptation of garter snakes to deadly prey. *Proceedings of the National Academy of Sciences*, *106*, 13415–13420.

Feldman, C. R., Brodie, E. D., Jr., Brodie, E. D., III, & Pfrender, M. E. (2010). Genetic architecture of a feeding adaptation: Garter snake (*Thamnophis*) resistance to tetrodotoxin bearing prey. *Proceedings of the Royal Society B: Biological Sciences*, *277*, 3317–3325.

Foll, M., & Gaggiotti, O. (2008). A genome-scan method to identify selected loci appropriate for both dominant and codominant markers: A Bayesian perspective. *Genetics*, *180*, 977–993.

Fukuda, M., Ujiie, R., Inoue, T., Chen, Q., Cao, C., Ding, L., Mori, N., & Mori, A. (2021). Do predators prefer toxic animals? A case of chemical discrimination by an Asian snake that sequesters firefly toxins. *Current Zoology*. https://doi.org/10.1093/cz/zoab102

Gall, B. G., Stokes, A. N., French, S. S., Schlepphorst, E. A., Brodie, E. D., III, & Brodie, E. D., Jr. (2011). Tetrodotoxin levels in larval and metamorphosed newts (*Taricha granulosa*) and palatability to predatory dragonflies. *Toxicon*, *57*, 978–983.

Gamberale-Stille, G., & Guilford, T. (2003). Contrast versus colour in aposematic signals. *Animal Behaviour*, *65*, 1021–1026.

Geffeney, S., Brodie, E. D., Jr., Ruben, P. C., & Brodie, E. D., III. (2002). Mechanisms of adaptation in a predator-prey arms race: TTX-resistant sodium channels. *Science*, *297*, 1336–1339.

Geffeney, S. L., Fujimoto, E., Brodie, E. D., III, Brodie, E. D., Jr., & Ruben, P. C. (2005). Evolutionary diversification of TTX-resistant sodium channels in a predator-prey interaction. *Nature*, *434*, 759–763.

Gendreau, K. L., Hague, M. T. J., Feldman, C. R., Brodie, E. D., Jr., Brodie, E. D., III, & McGlothlin, J. W. (2020). Sex linkage of the skeletal muscle sodium channel gene (SCN4A) explains apparent deviations from hardy–Weinberg equilibrium of tetrodotoxin-resistance alleles in garter snakes (*Thamnophis sirtalis*). *Heredity*, *124*, 647–657.

Goudet, J., & Jombart, T. (2015). hierfstat: Estimation and tests of hierarchical F-statistics.

Groen, S. C., & Whiteman, N. K. (2021). Convergent evolution of cardiac-glycoside resistance in predators and parasites of milkweed herbivores. *Current Biology*, *31*, R1465–R1466.

Gruber, B., Unmack, P. J., Berry, O. F., & Georges, A. (2018). dartr: An R package to facilitate analysis of SNP data generated from reduced representation genome sequencing. *Molecular Ecology Resources*, *18*, 691–699.

Guimarães, P. R., Pires, M. M., Jordano, P., Bascompte, J., & Thompson, J. N. (2017). Indirect effects drive coevolution in mutualistic networks. *Nature*, *550*, 511–514.

Hague, M. T., Stokes, A. N., Feldman, C. R., Brodie, E. D., Jr., & Brodie, E. D., III. (2020a). The geographic mosaic of arms race coevolution is closely matched to prey population structure. *Evolution Letters*, *4*, 317–332.

Hague, M. T. J., Avila, L. A., Hanifin, C. T., Snedden, W. A., Stokes, A. N., Brodie, E. D., Jr., & Brodie, E. D., III. (2016). Toxicity and population structure of the Rough-Skinned Newt (*Taricha granulosa*) outside the range of an arms race with resistant predators. *Ecology and Evolution*, *6*, 2714–2724.

Hague, M. T. J., Feldman, C. R., Brodie, E. D., Jr., & Brodie, E. D., III. (2017). Convergent adaptation to dangerous prey proceeds through the same first-step mutation in the garter snake Thamnophis sirtalis. *Evolution*, *71*, 1504–1518.

Hague, M. T. J., Stokes, A. N., Feldman, C. R., Brodie, E. D., Jr., & Brodie, E. D., III. (2020b). Data from: The geographic mosaic of arms race coevolution is closely matched to prey population structure. *Dryad, Dataset*. https://doi.org/10.5061/dryad.51c59zw5k

Hague, M. T. J., Toledo, G., Geffeney, S. L., Hanifin, C. T., Brodie, E. D., Jr., & Brodie, E. D., III. (2018). Large-effect mutations generate trade-off between predatory and locomotor ability during arms race coevolution with deadly prey. *Evolution Letters*, *2*, 406–416.

Hanifin, C. T., Brodie, E. D., III, & Brodie, E. D., Jr. (2002). Tetrodotoxin levels of the rough-skin newt, *Taricha granulosa*, increase in long-term captivity. *Toxicon*, *40*, 1149–1153.

Hanifin, C. T., Brodie, E. D., III, & Brodie, E. D., Jr. (2004). A predictive model to estimate total skin tetrodotoxin in the newt *Taricha granulosa*. *Toxicon*, *43*, 243–249.

Hanifin, C. T., Brodie, E. D., Jr., & Brodie, E. D., III. (2008). Phenotypic mismatches reveal escape from arms-race coevolution. *PLoS Biology*, *6*, e60.

Hutchinson, D. A., Mori, A., Savitzky, A. H., Burghardt, G. M., Wu, X., Meinwald, J., & Schroeder, F. C. (2007). Dietary sequestration of defensive steroids in nuchal glands of the Asian snake *Rhabdophis tigrinus*. *Proceedings of the National Academy of Sciences*, *104*, 2265–2270.

Hutchinson, D. A., Savitzky, A. H., Mori, A., Burghardt, G. M., Meinwald, J., & Schroeder, F. C. (2012). Chemical investigations of defensive steroid sequestration by the Asian snake *Rhabdophis tigrinus*. *Chemoecology*, *22*, 199–206.

Jackson, J. F., Ingram, W., III, & Campbell, H. W. (1976). The dorsal pigmentation pattern of snakes as an antipredator strategy: A multivariate approach. *The American Naturalist*, *110*, 1029–1053.

Janzen, F. J., Krenz, J. G., Haselkorn, T. S., Brodie, E. D., Jr., & Brodie, E. D., III. (2002). Molecular phylogeography of common garter snakes (*Thamnophis sirtalis*) in western North America: Implications for regional historical forces. *Molecular Ecology*, *11*, 1739–1751.

Karageorgi, M., Groen, S. C., Sumbul, F., Pelaez, J. N., Verster, K. I., Aguilar, J. M., Hastings, A. P., Bernstein, S. L., Matsunaga, T., Astourian, M., Guerra, G., Rico, F., Dobler, S., Agrawal, A. A., & Whiteman, N. K. (2019). Genome editing retraces the evolution of toxin resistance in the monarch butterfly. *Nature*, *574*, 409–412.

Langmead, B., & Salzberg, S. L. (2012). Fast gapped-read alignment with Bowtie 2. *Nature Methods*, *9*, 357–359.

Lynch, M., & Walsh, B. (1998). *Genetics and analysis of quantitative traits*. Sinauer.

Maia, R., Eliason, C. M., Bitton, P.-P., Doucet, S. M., & Shawkey, M. D. (2013). pavo: An R package for the analysis, visualization and organization of spectral data. *Methods in Ecology and Evolution*, *4*, 906–913.

Mason, R. T., Fales, H. M., Jones, T. H., Pannell, L. K., Chinn, J. W., & Crews, D. (1989). Sex pheromones in snakes. *Science*, *245*, 290–293.

Mason, R. T., & Parker, M. R. (2010). Social behavior and pheromonal communication in reptiles. *Journal of Comparative Physiology. A, Neuroethology, Sensory, Neural, and Behavioral Physiology*, *196*, 729–749.

Mochida, K. (2009). A parallel geographical mosaic of morphological and behavioural aposematic traits of the newt, *Cynops pyrrhogaster* (Urodela: Salamandridae). *Biological Journal of the Linnean Society*, *97*, 613–622.

Mori, A., Burghardt, G. M., Savitzky, A. H., Roberts, K. A., Hutchinson, D. A., & Goris, R. C. (2012). Nuchal glands: A novel defensive system in snakes. *Chemoecology*, *22*, 187–198.

Motychak, J. E., Brodie, E. D., Jr., & Brodie, E. D., III. (1999). Evolutionary response of predators to dangerous prey: Preadaptation and the evolution of tetrodotoxin resistance in garter snakes. *Evolution*, *53*, 1528–1535.

Opitz, S. E., & Müller, C. (2009). Plant chemistry and insect sequestration. *Chemoecology*, *19*, 117–154.

Pembleton, L. W., Cogan, N. O. I., & Forster, J. W. (2013). StAMPP: An R package for calculation of genetic differentiation and structure of mixed-ploidy level populations. *Molecular Ecology Resources*, *13*, 946–952.

Perry, B. W., Card, D. C., McGlothlin, J. W., Pasquesi, G. I., Adams, R. H., Schield, D. R., Hales, N. R., Corbin, A. B., Demuth, J. P., Hoffmann, F. G., Vandewege, M. W., Schott, R. K., Bhattacharyya, N., Chang, B. S. W., Casewell, N. R., Whiteley, G., Reyes-Velasco, J., Mackessy, S. P., Gamble, T., … Castoe, T. A. (2018). Molecular adaptations for sensing and securing prey and insight into amniote genome diversity from the garter snake genome. *Genome Biology and Evolution*, *10*, 2110–2129.

Peterson, B. K., Weber, J. N., Kay, E. H., Fisher, H. S., & Hoekstra, H. E. (2012). Double digest RADseq: An inexpensive method for de novo SNP discovery and genotyping in model and non-model species. *PLoS One*, *7*, e37135–e37111.

Petschenka, G., & Agrawal, A. A. (2015). Milkweed butterfly resistance to plant toxins is linked to sequestration, not coping with a toxic diet. *Proceedings of the Royal Society B: Biological Sciences*, *282*, 20151865.

Petschenka, G., Halitschke, R., Züst, T., Roth, A., Stiehler, S., Tenbusch, L., Hartwig, C., Moreno Gámez, J. F., Trusch, R., Deckert, J., Chalušová, K., Vilcinskas, A., & Exnerová, A. (2022). Sequestration of defenses against predators drives specialized host plant associations in preadapted milkweed bugs (Heteroptera: Lygaeinae). *The American Naturalist*, *199*, E211–E228.

Pfennig, D. W., & Mullen, S. P. (2010). Mimics without models: Causes and consequences of allopatry in Batesian mimicry complexes. *Proceedings of the Royal Society B: Biological Sciences*, *277*, 2577–2585.

R Core Team. (2022). *R: A language and environment for statistical computing*. R Foundation for Statistical Computing.

Rambaut, A., Suchard, M., Xie, D., & Drummond, A. (2014). Tracer.

Reimche, J. S., Brodie, E. D., Jr., Stokes, A. N., Ely, E. J., Moniz, H. A., Thill, V. L., Hallas, J. M., Pfrender, M. E., Brodie, E. D., III, & Feldman, C. R. (2020). The geographic mosaic in parallel: Matching patterns of newt tetrodotoxin levels and snake resistance in multiple predator–prey pairs. *Journal of Animal Ecology*, *89*, 1645–1657.

Ridenhour, B. J., Brodie, E. D., III, & Brodie, E. D., Jr. (2004). Resistance of neonates and field-collected garter snakes (*Thamnophis* spp.) to tetrodotoxin. *Journal of Chemical Ecology*, *30*, 143–154.

Roper, T. (1990). Responses of domestic chicks to artificially coloured insect prey: Effects of previous experience and background colour. *Animal Behaviour*, *39*, 466–473.

Rossman, D. A., Ford, N. B., & Seigel, R. A. (1996). *The garter snakes: Evolution and ecology* (1st ed.). University of Oklahoma Press.

Schneider, C. A., Rasband, W. S., & Eliceiri, K. W. (2012). NIH image to ImageJ: 25 years of image analysis. *Nature Methods*, *9*, 671–675.

Scordato, E. S., Wilkins, M. R., Semenov, G., Rubtsov, A. S., Kane, N. C., & Safran, R. J. (2017). Genomic variation across two barn swallow hybrid zones reveals traits associated with divergence in sympatry and allopatry. *Molecular Ecology*, *26*, 5676–5691.

Shine, R., Olsson, M. M., Lemaster, M. P., Moore, I. T., & Mason, R. T. (2000). Effects of sex, body size, temperature, and location on the antipredator tactics of free-ranging gartersnakes (*Thamnophis sirtalis*, Colubridae). *Behavioral Ecology*, *11*, 239–245.

St. John, A. (2002). *Reptiles of the northwest: California to Alaska; Rockies to the coast*. Lone Pine.

Stebbins, R. C. (2003). *A field guide to Western reptiles and amphibians* (3rd ed.). Houghton Mifflin Harcourt.

Stokes, A. N., Ray, A. M., Buktenica, M. W., Gall, B. G., Paulson, E., Paulson, D., French, S. S., Brodie, E. D., III, & Brodie, E. D., Jr. (2015). Otter predation on *Taricha granulosa* and variation in tetrodotoxin levels with elevation. *Northwestern Naturalist*, *96*, 13–21.

Stokes, A. N., Williams, B. L., & French, S. S. (2012). An improved competitive inhibition enzymatic immunoassay method for tetrodotoxin quantification. *Biological Procedures*, *14*, 3.

Sweet, S. S. (1985). Geographic variation, convergent crypsis and mimicry in gopher snakes (*Pituophis melanoleucus*) and western rattlesnakes (*Crotalus viridis*). *Journal of Herpetology*, *19*, 55–67.

Thompson, J. N. (1999). Specific hypotheses on the geographic mosaic of coevolution. *The American Naturalist*, *153*, S1–S14.

Thompson, J. N. (2005). *The geographic mosaic of coevolution*. University of Chicago Press.

Toju, H., & Sota, T. (2005). Imbalance of predator and prey armament: Geographic clines in phenotypic interface and natural selection. *The American Naturalist*, *167*, 105–117.

Toju, H., Ueno, S., Taniguchi, F., & Sota, T. (2011). Metapopulation structure of a seed-predator weevil and its host plant in arms race coevolution. *Evolution*, *65*, 1707–1722.

Venesky, M. D., & Anthony, C. D. (2007). Antipredator adaptations and predator avoidance by two color morphs of the eastern red-backed salamander, *Plethodon cinereus*. *Herpetologica*, *63*, 450–458.

Vermeij, G. J. (1987). *Evolution and escalation: An ecological history of life*. Princeton University Press.

Vicoso, B., Emerson, J., Zektser, Y., Mahajan, S., & Bachtrog, D. (2013). Comparative sex chromosome genomics in snakes: Differentiation, evolutionary strata, and lack of global dosage compensation. *PLoS Biology*, *11*, e1001643.

Westphal, M. F. (2007). *On the evolution of correlated color traits in garter snakes*. Oregon State University.

Westphal, M. F., Massie, J. L., Bronkema, J. M., Smith, B. E., & Morgan, T. J. (2011). Heritable variation in garter snake color patterns in postglacial populations. *PLoS One*, *6*, e24199.

Westphal, M. F., & Morgan, T. J. (2010). Quantitative genetics of pigmentation development in 2 populations of the common garter snake, *Thamnophis sirtalis*. *The Journal of Heredity*, *101*, 573–580.

Williams, B. L., Brodie, E. D., Jr., & Brodie, E. D., III. (2003). Coevolution of deadly toxins and predator resistance: Self-assessment of resistance by garter snakes leads to behavioral rejection of toxic newt prey. *Herpetologica*, *59*, 155–163.

Williams, B. L., Brodie, E. D., Jr., & Brodie, E. D., III. (2004). A resistant predator and its toxic prey: Persistence of newt toxin leads to poisonous (not venomous) snakes. *Journal of Chemical Ecology*, *30*, 1901–1919.

Williams, B. L., Hanifin, C. T., Brodie, E. D., Jr., & Brodie, E. D., III. (2012). Predators usurp prey defenses? Toxicokinetics of tetrodotoxin in common garter snakes after consumption of rough-skinned newts. *Chemoecology*, *22*, 179–185.

Yoshida, T., Ujiie, R., Savitzky, A. H., Jono, T., Inoue, T., Yoshinaga, N., Aburaya, S., Aoki, W., Takeuchi, H., Ding, L., Chen, Q., Cao, C., Tsai, T.-S., de Silva, A., Mahaulpatha, D., Nguyen, T. T., Tang, Y., Mori, N., & Mori, A. (2020). Dramatic dietary shift maintains sequestered toxins in chemically defended snakes. *Proceedings of the National Academy of Sciences*, *117*, 5964–5969.

Zaman, L., Meyer, J. R., Devangam, S., Bryson, D. M., Lenski, R. E., & Ofria, C. (2014). Coevolution drives the emergence of complex traits and promotes evolvability. *PLoS Biology*, *12*, e1002023-9.

Zangerl, A. R., & Berenbaum, M. R. (2003). Phenotype matching in wild parsnip and parsnip webworms: Causes and consequences. *Evolution*, *57*, 806–815.

SUPPORTING INFORMATION

Additional supporting information can be found online in the Supporting Information section at the end of this article.

How to cite this article: Hague, M. T. J., Miller, L. E., Stokes, A. N., Feldman, C. R., Brodie, E. D. Jr, & Brodie, E. D. III (2022). Conspicuous coloration of toxin-resistant predators implicates additional trophic interactions in a predator–prey arms race. *Molecular Ecology*, *00*, 1–15. https://doi.org/10.1111/mec.16772